IEEE Access
Multidisciplinary | Rapid Review | Open Access Journal

Received April 27, 2018, accepted May 29, 2018, date of publication June 18, 2018, date of current version July 19, 2018.

Digital Object Identifier 10.1109/ACCESS.2018.2846260

Spatial Correlation Models of Large-Scale Antenna Topologies Using Maximum Power of Offset Distribution and Its Application

AFFUM EMMANUEL AMPOMA[1,2], GUANGJUN WEN[1], YONGJUN HUANG[1], KWAME OTENG GYASI[1], PARFAIT I. TEBE[1], AND KWADWO NTIAMOAH-SARPONG[1]

[1]Center for RFIC and System Technology, University of Electronic Science and Technology of China, Chengdu 611731, China
[2]Electrical and Electronic Department, Kwame Nkrumah University of Science and Technology, Kumasi, Ghana

Corresponding author: Affum Emmanuel Ampoma (ampoma.uestc@yahoo.com)

This work was supported in part by the National Natural Science Foundation of China under Project 61601093, Project 61791082, and Project 61701116, in part by the Sichuan Provincial Science and Technology Planning Program of China under Project 2016GZ0061 and Project 18GJHZ0044, in part by the Fundamental Research Funds for the Central Universities under Project ZYGX2016Z011, and in part by the Science and Technology on Electronic Information Control Laboratory.

ABSTRACT

In this paper, we present an approximate expression for spatial correlation of cylindrical and uniform rectangular arrays regarding the maximum power of offset distributions useful for evaluating geometry-based stochastic channel models. The underlying concept of the proposed spatial correlation expression is that the maximum power of arrival varies relative to the offset distribution in the azimuth and zenith domains. Verification is accomplished with the help of computer simulation, where perfect agreement between theoretical and Monte Carlo simulation results is found. Toward the implementation of large-scale MIMO transmitters in constrained physical spaces to accomplish the demands for the next generation of wireless systems, we examine the effect of the proposed spatial correlation model on the downlink (DL) performance of massive multi-input-multi-output (MIMO) system. Results illustrate that the DL capacity does not demonstrate any sensitivity to the effect of correlation by increasing the number of elements in a realistic massive MIMO channel. Surprisingly, while the spatial correlation restricts the DL capacity at a reduced number of transmit antennas, the restriction becomes insignificant as the number of transmit antennas increases. This supports existing developments that user channels decorrelate when the number of antennas at the base station increases. Finally, experimental results show that separation of more than half wavelength is inadequate to decorrelate the antenna elements.

INDEX TERMS Antenna arrays, cluster model, massive MIMO, maximum power of arrival (MPA), small cell network (SCN), spatial correlation (SC).

I. INTRODUCTION

Recently research on antenna arrays has attracted attention among researchers in the communication industries. This is because antenna arrays determine the spatial correlation (SC), mutual coupling and channel characteristics, furthering the capacity of MIMO system [1]. The MIMO technologies have remained a topic of significance in wireless communication due to the substantial gains they offer concerning spectral efficiency [2]. However, the resulting need for increasing the number of antenna elements in a restricted physical space to achieve higher transmission rate and more considerable diversity creates two primary effects: spatial correlation (SC) owing to nearness (proximity) of antennas as signal sources and mutual coupling as a result of the proximity of the antenna elements as electrical components [1], [3], [4]. It has been demonstrated that it requires antenna separation up to tens of wavelengths at the transmitter to create uncorrelated sub-channels for higher performance [3]. This is because an efficient MIMO system is not only accomplished by increasing the number of transmitting and

receiving antennas, but the correlation between antenna elements must be minimized [5], [6]. Given this, investigations on antenna array architectures are valuable for the development of future MIMO technologies. In order to meet the demands for a higher transmission rate for future networks, the massive MIMO systems has been proposed [7], [8]. The massive MIMO system depends on having a substantial number of antennas at each base station (BS) and exploiting channel reciprocity in time division duplex mode (TDD) [13]. Apart from increasing data rates, the massive MIMO system is expected to provide larger network capacity, higher spectral efficiency and higher energy efficiency [7]. Other benefits are 1) mitigation of propagation losses by a large array gain as a result of coherent beamforming; 2) low-complexity signal processing algorithms are asymptotically optimal: and 3) inter-user interference is easily mitigated by the high beamforming resolution [13]. To meet these requirements, Hoydis *et al.* [9], Liu *et al.* [10], and Zheng *et al.* [11] have established that the small cell network (SCN) and the three-dimensional (3-D) MIMO with large-scale antennas are the promising techniques in providing high spectral efficiency (SE) for the massive MIMO system [7], [9]–[13].

The SCN is made up of densely deployed low-cost and low-power BSs with an improved cell-splitting gain. SCN reduces the separation between the transmitters and receivers and minimizes the required transmit power to overcome path loss [9]. In addition, the SCN closes the BSs with low traffics for energy saving to enhance performance [9]. On the other hand, the benefits of the 3-D MIMO with large-scale antennas are higher data rate, greater spectrum efficiency, larger average throughput and shorter latency [8]. Another advantage is that the 3-D MIMO can exploit the degree of large-scale antennas to enhance performance [11]. Besides, the horizontal and vertical dimensions of the beam of these transmit antennas can be adjusted to improve signal power and reduce inter-cell interference [14].

The practical implementation of 3-D MIMO with large-scale antennas in an SCN will result in a limited available physical space at the BS that will hinder the deployment of large numbers of antenna elements [4]. This will reduce the inter-element spacing between elements as signal sources and bring about considerable SC, and subsequently reduce the channel capacity. Massive MIMO communication is widely investigated, however, with the possibility of a large number of antennas in SCN, it is desirable to accurately characterize the SC of large-scale antenna arrays for an efficient design to evaluate massive MIMO systems regarding 3GPP standards. In addition, in consideration of the advantages of the 3-D MIMO for the deployment of massive MIMO [11], it is, therefore, reasonable to examine the effect of correlation on massive MIMO systems regarding channel models when different antenna topologies represent the BS.

Different types of large-scale antenna architectures have been proposed for the massive MIMO system [11]. In this analysis, we consider cylindrical array (CA) and uniform rectangular array (URA). This is because the radiated MIMO signals from these arrays can be well regulated in the 3-D space to improve the system capacity [11], [14]. In addition, the CA can be employed as a means of clutter suppression via scanning acceleration and space-time signal [15]. Also, the CA permits the possibility to either generate directed beams in an arbitrary direction in the horizontal plane or to produce an omnidirectional pattern [16].

The amount of research on SC of antenna arrays has increased rapidly, but the effects of SC of the large-scale antennas on massive MIMO system has received little attention. For SC of large-scale antenna arrays using cluster model, many refer to the works in [17], where authors presented an approximate SC model of the uniform circular array (UCA) and the uniform linear array (ULA) in the azimuth domain. The model did not consider the zenith domain because most of the energy is localized over the azimuth directions when the angle-of-arrival (AOA) and angle-of-departure (AOD) are physically distributed over the 3-D space [17]. Ying *et al.* [18] have shown that the SC matrix can be expressed as the Kronecker product of each correlation matrix in the azimuth and zenith directions. Following this development, approximate expressions for SC of CA and URA in azimuth and zenith domains have been developed using Fourier transforms to investigate the convergence properties of correlated channels [19]. Nevertheless, the numerical outcomes to show the variation between correlation coefficients regarding antenna separation were not included in the analysis.

With the likelihood of confined large-scale antenna array dimensions in SCN and the adverse impact of SC on massive MIMO system performance. This paper focuses on developing approximate SC expressions of CA and URA regarding the maximum power of offset distribution. This is to investigate the effects of SC on the performance of massive MIMO using 3GPP standards which follow geometry-based stochastic models described in [20].

The maximum power of arrival (MPA) concept was first defined in [21]. The idea was developed to derive the 3D SC of URA for analyzing the dependency of MIMO channel capacity and bit error rate on azimuth and elevation spreads [22]. With progress in MIMO innovation, other efficient methods of characterizing the SC of antenna arrays are required. The MPA strategy gives a standard guideline for assessing the SC of CA and URA concerning different angular distributions. Moreover, the MPA concept streamlines the computation of the SC and avoids the need to generate distinct expressions for CA and URA for evaluating next generation of wireless systems [22].

Given this, we follow the guidelines in [19] and make small angle approximations to precisely determine the SC expressions of CA and URA regarding the MPA of offset distributions in the azimuth and zenith domains. Moreover, Bjornson *et al.* [13] have indicated that user channels in massive MIMO decorrelate when the number of antennas at the BS increases, thus strong signal gains are achievable with little interuser interference. However, the DL capacity

analysis in [13] considered spatially uncorrelated channels. Again, the conventional flat-fading multiple-input single output (MISO) DL channel considered in the investigations do not accurately reflect the realistic channel properties and is more unsuitable for evaluating massive MIMO system [11]. Evaluating the DL performance of practical wireless communication systems requires a channel model that accurately comprise the channel properties and incorporates large-scale parameters (e.g., delay and angular spreads) and small-scale parameters (e.g., delays, cluster powers, and arrival- and departure angles). Therefore, the need to investigate the DL performance of massive MIMO systems by incorporating the effects of SC between antenna elements in a realistic channel is considered warranted.

For reasons of clarity, the objectives of this paper are in two-fold: First is to derive an approximate expression for SC of CA and URA regarding the MPA of offset distributions in the azimuth and zenith domains, and second is to validate the proposed SC expression using geometry-based stochastic models. We provide results to indicate that there is a perfect agreement between theoretical and Monte Carlo simulation results, in spite of the numerical evaluation. For validation, we follow the guidelines in [23] and present a relating channel model of the WINNER+ and 3GPP standard in [20] when CA and URA represent BS. To illustrate the effects of correlation, we concentrate on the DL performance and present the correlated model of the uncorrelated DL upper bound capacity (in bits/channel use) limits based on perfect CSI in [13]. Our outcome demonstrates that the DL capacity does not respond to the effect of correlation by increasing antenna elements at the BS. Even though increasing the number of antennas at the BS reduces the separation between antenna elements and increases correlation. We observed that while the SC restricts the DL capacity by reducing the number of antennas at the BS, the restriction is relaxed by increasing the number of antennas at the BS. This also supports the existing development that user channels decorrelate when the number of antennas at the BS increases to enhance performance [13].

The rest of the paper is organized as follows: we present the concept of the MPA of offset distribution and derive the SC of CA and URA in Section II. Section III presents the antenna configuration and the 3-D channel modeling. The system model is presented in Section IV. Section V focuses on numerical results, and Section VI concludes the paper.

II. MAXIMUM POWER OF ARRIVAL AND SPATIAL CORRELATION

A. MAXIMUM POWER OF OFFSET DISTRIBUTION

In this section, we present the MPA concept regarding offset distribution and derive the SC expressions of CA and URA. The cluster model is shown in *Figure 1*, where multiple scatterers around the receive array are modeled as clusters [17]. The array is located on the z-axis, $\Delta\theta$ is the zenith AOA/AOD offset relative to its mean AOA, θ [19]. Also, if the antenna

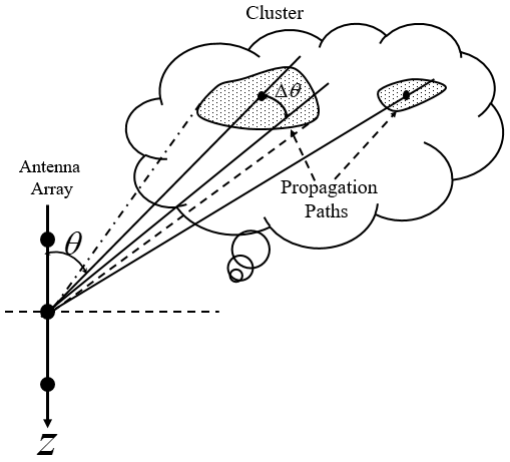

FIGURE 1. Geometry of cluster model and propagation paths.

array was situated on the y-axis, the offset azimuth AOD can be represented by $\Delta\phi$ relative to its mean AOD, ϕ.

Definition [Maximum Power of Offset Distribution]: If $p(u)$ is the true distribution of power as a function of $u = \sin(\alpha)$, where α is the phase of the incident wave, then the MPA is relative to the distribution of true power and it is given as [22] and [23] $P_{max} = \int_u p(u)\,\mathrm{d}u$.

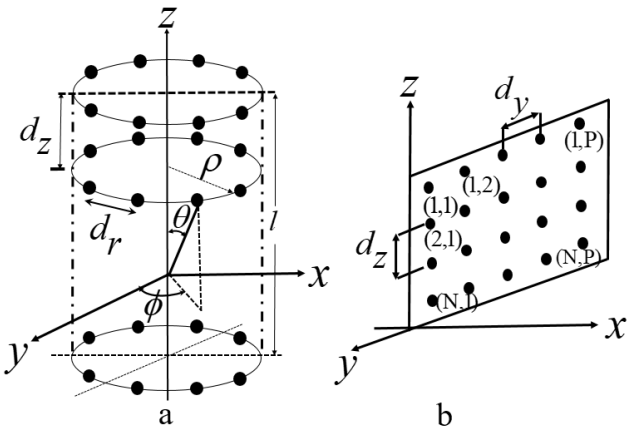

FIGURE 2. Geometry of (a) cylindrical array (b) rectangular array.

B. PROPOSED SPATIAL CORRELATION OF CYLINDRICAL AND RECTANGULAR ARRAYS

The CA is shown in *Figure 2a* and can be achieved by wrapping a URA around a virtual cylinder. In this analysis, the CA is modeled as a A element ULA in the z domain [19] and B element UCA on the $x-$ and $y-$ planes (azimuth domain). The SC of CA can be expressed as [18]

$$R = R_\phi \otimes R_\theta \tag{1}$$

where R_ϕ and R_θ are the azimuth and zenith domains correlation, respectively. $\otimes$ is the Kronecker product. The R_ϕ

between *ath* and $a'th$ antenna is given as [19]

$$R_{\phi(a,a')} = \iint e^{j[\Phi_a(\Delta\phi,\Delta\theta)-\Phi_{a'}(\Delta\phi,\Delta\theta)]} \times p_{\Delta\phi}(\Delta\phi)p_{\Delta\theta}(\Delta\theta)\mathrm{d}\Delta\phi\Delta\theta \quad (2)$$

where $\Delta\phi$ is the azimuth domain AOA offset relative to its mean, ϕ. $\Delta\theta$ is the zenith domain AOA offset relative to its mean, θ. $\Phi(\Delta\phi, \Delta\theta)$ is the phase shift of *ath* antenna in the azimuth domain and is expressed as [19]

$$\Phi(\Delta\phi, \Delta\theta) = k\rho a\cos((\phi-\phi_a)+\Delta\theta)\sin(\theta+\Delta\theta) \quad (3)$$

where k and ρ are the wave number and the radius of CA, respectively. To achieve the approximate expression of SC in the azimuth domain, we follow the guidelines in [19] to expand Eq. (3) to introduce the azimuth domain distribution factor $\Delta\phi$ as an independent variable into the phase shift expression that can significantly influence the azimuth domain correlation $R_{\phi(a,a')}$. According to [19] the first-order Taylor series of $\cos((\phi-\phi_b)+\Delta\phi)$, while assuming $\Delta\phi \approx 0$ is given as $\cos((\phi-\phi_b)+\Delta\phi) \approx \cos(\phi-\phi_b) - \Delta\phi\sin(\phi-\phi_b)$. Therefore, Eq. (3) becomes

$$k\rho a\cos((\phi-\phi_a)+\Delta\phi)\sin(\theta+\Delta\theta) \approx k\rho a\sin(\theta+\Delta\theta)\times[\cos(\phi-\phi_a)-\Delta\phi\sin(\phi-\phi_a)] \quad (4)$$

Substituting Eq. (4) into Eq. (2), the SC becomes

$$R_{\phi(a,a')} \approx \iint e^{jk\rho(a-a')\sin(\theta+\Delta\theta)[\cos(\phi-\phi_a)-\Delta\phi\sin(\phi-\phi_a)]} \times p_{\Delta\phi}(\Delta\phi)p_{\Delta\theta}(\Delta\theta)\mathrm{d}\Delta\phi\mathrm{d}\Delta\theta \quad (5)$$

Letting $x = k\rho(a-a')[\cos(\phi-\phi_a)-\Delta\phi\sin(\phi-\phi_a)]$ and $\omega = (\theta+\Delta\theta)$, we rewrite Eq. (5) as

$$R_{\phi(a,a')} = \int_{-\pi}^{\pi}\int_{-\pi}^{\pi} e^{jx\sin(\omega)}P_{\Delta\phi}(\Delta\phi)P_{\Delta\theta}(\Delta\theta)\mathrm{d}\Delta\phi\Delta\theta \quad (6)$$

Motivated by the above definition, the SC regarding the MPA of offset distribution becomes

$$R_{\phi(a,a')} = P_{\Delta\phi,\Delta\theta}(\Delta\phi,\Delta\theta)_{max}\int_{-\pi}^{\pi}\int_{-\pi}^{\pi} e^{jx\sin(\omega)}\mathrm{d}\Delta\phi\Delta\theta \quad (7)$$

For independent probability density functions, we assume that the effective MPA can be expressed as [19]

$$P_{\Delta\phi,\Delta\theta}(\Delta\phi,\Delta\theta)_{max} = P^{azi}_{\Delta\phi max}(\Delta\phi)P^{ze}_{\Delta\theta max}(\Delta\theta) \quad (8)$$

where $P^{azi}_{\Delta\phi max}(\Delta\phi)$ and $P^{ze}_{\Delta\theta max}(\Delta\theta)$ are the MPA of offset distribution in the azimuth and zenith domains, respectively, and are evaluated in Section II (D).

We evaluate Eq. (7) using the Bessel substitutions in [22], [24], and [25]

$$J_o(x) = \frac{1}{2}\int_{-\pi}^{\pi} e^{-j(n\omega-x\sin(\omega))}d\omega \overbrace{=}^{n=0} \frac{1}{2\pi}\int_{-\pi}^{\pi} e^{jx\sin(\omega)}d\omega \quad (9)$$

for two periodical functions integrated over 2π, Eq. (9) can be expressed as [22] and [25]

$$J_0(x) = \frac{1}{2\pi}\int_0^{2\pi} e^{jx\cos(\omega)}d\omega \quad (10)$$

Substituting Eq. (9) into Eq. (7)

$$R_{\phi(a,a')} = 2\pi P_{\Delta\phi,\Delta\theta}(\Delta\phi,\Delta\theta)_{max} \times\int_{-\pi}^{\pi}\left\{\frac{1}{2\pi}\int_{-\pi}^{\pi} e^{jx\sin(\omega)}\mathrm{d}\Delta\theta\right\}\mathrm{d}\Delta\phi \quad (11)$$

$$R_{\phi(a,a')} = 4\pi P_{\Delta\phi,\Delta\theta}(\Delta\phi,\Delta\theta)_{max}\int_0^{\pi} J_0(x)\mathrm{d}\Delta\phi \quad (12)$$

With specific solutions such as [22] and [24]

$$\int_0^{\pi} J_0(x\sin(\phi))\sin(\phi)\mathrm{d}\phi = \sqrt{(2\pi/x)}J_{1/2}(x), \quad x \geq 0 \quad (13)$$

and $J_{1/2}(x) = \sqrt{(2/\pi x)}\sin(x), x \geq 0$. Comparing Eqs. (12) and (13), the SC in the azimuth domain of CA is approximated as

$$R_{\phi(a,a')} \approx \frac{4\pi P_{\Delta\phi,\Delta\theta(\Delta\phi,\Delta\theta)_{max}}}{x\cos(\phi)}\sin(x) \quad (14)$$

In zenith domain correlation, R_θ is expressed as [19]

$$R_{\theta(b,b')} = \int e^{j[\psi_b(\Delta\theta)-\psi_{b'}(\Delta\theta)]}p_{\Delta\theta}(\Delta\theta)\mathrm{d}\Delta\theta \quad (15)$$

where $\psi_b(\Delta\theta) = kd_z\cos(\theta+\Delta\theta)$ is the phase shift of *bth* antenna is the zenith domain [19]. Substituting $\psi_b(\Delta\theta)$, Eq. (15) can be written as

$$R_{\theta(b,b')} \approx 2\int_0^{\pi} e^{jkd_z(b-b')[\cos(\theta+\Delta\theta)]}p_{\Delta\theta}(\Delta\theta)\mathrm{d}\Delta\theta \quad (16)$$

Letting $x = kd_z(b-b')$ and $\omega = \theta+\Delta\theta$ for two periodical functions integrated over 2π, Eq. (16) becomes

$$R_{\theta(b,b')} = 4\pi\left(\frac{1}{2\pi}\int_0^{2\pi} e^{jx\cos(\omega)}p_{\Delta\theta}(\Delta\theta)\mathrm{d}\Delta\theta\right) \quad (17)$$

Using Eqs.(9) and (10), the SC regarding the MPA of offset distribution in the zenith domain can be written as

$$R_{\theta(b,b')} = 4\pi P_{max}{}^{ze}_{\Delta\theta}\left(\frac{1}{2\pi}\int_{-\pi}^{\pi} e^{jx\sin(\omega)}\mathrm{d}\Delta\theta\right) = 4\pi P_{max}{}^{ze}_{\Delta\theta}J_0(kd_z(b-b')) \quad (18)$$

On account of URA shown in *Figure 2b*. The azimuth phase shift of the *ath* antenna element to the reference antenna is expressed as [19]

$$\Phi_b(\Delta\phi,\Delta\theta) = kd_y\cos(\phi+\Delta\phi)\sin(\theta+\Delta\theta) \quad (19)$$

This is equivalent to that of CA in Eq. (3), when $d_y = \rho$ and $\phi = \phi-\phi_b$ [19]. Given this, the $R_{\theta(a,a')}$ expression of URA is equal to the $R_{\phi(a,a')}$ expression of CA in Eq. (14). The zenith phase shift of the *bth* antenna element of URA is identical to that of CA and the SC expression is the same as in Eq. (18) [19].

C. MAXIMUM POWER USING 3GPP MEASURED VALUES

We now proceed to evaluate the MPA of offset distributions using the 3GPP measured values in [26]. The azimuth and zenith AOA offsets are modeled as Wrapped Gaussian and Laplacian distributions, respectively. The Wrapped Gaussian distribution is expressed as [19] and [26]

$$p_{\Delta\phi}(\Delta\phi) = 1/\sigma_{\Delta\phi}\sqrt{2\pi}\sum_{i=-\infty}^{\infty} e^{-(\Delta\phi+2\pi i)^2/2\sigma_{\Delta\phi}} \quad (20)$$

The Laplacian distribution is expressed as

$$p_{\Delta\theta}(\Delta\theta) = \left(\kappa/\sigma_{\Delta\theta}\sqrt{2}\right) e^{-|\Delta\theta\sqrt{2}/\sigma_{\Delta\theta}|} \quad (21)$$

where the constant $\kappa = 1/\left(1 - e^{-\sqrt{2\pi}/\sigma_{\Delta\theta}}\right)$ normalizes the PDF, $\sigma_{\Delta\phi}$ and $\sigma_{\Delta\theta}$ are the standard deviations (SD) of AOA offsets $\Delta\phi$ and $\Delta\theta$, respectively. Both distributions are zero outside the range $[-\pi, \pi]$. Motivated by the above definition, the MPA in the azimuth domain is given as

$$P^{azi}_{\Delta\theta max} = \frac{1}{\sigma_{\Delta\phi}\sqrt{2\pi}}\sum_{i=-\infty}^{\infty}\int e^{-(\Delta\phi+2\pi i)^2/2\sigma^2_{\Delta\phi}}\mathrm{d}\Delta\phi \quad (22)$$

$$P^{azi}_{\Delta\theta max} = \frac{\sigma_{\Delta\phi}}{\sqrt{2\pi}}\sum_{i=-\infty}^{\infty}\frac{-1}{(\Delta\phi+2\pi i)}e^{-(\Delta\phi+2\pi i)^2/2\sigma^2_{\Delta\phi}} \quad (23)$$

Likewise, the MPA in zenith domain is given as

$$\begin{aligned} P^{ze}_{\Delta\theta max} &= \frac{\kappa}{\sigma_{\Delta\theta}\sqrt{2}}\int e^{-|\Delta\theta\sqrt{2}/\sigma_{\Delta\theta}|}\mathrm{d}\Delta\theta \\ &= -\frac{\kappa}{2}e^{-|\Delta\theta\sqrt{2}/\sigma_{\Delta\theta}|} \end{aligned} \quad (24)$$

Substituting Eqs. (14) and (18) into Eq. (1), and using the well-known series of $\sin(\theta)$ and $\cos(\theta)$, the SC expression of CA and URA concerning Bessel functions regarding the MPA of offset distribution is expressed as

$$\begin{aligned} R = {} & 2\sum_{k=0}^{\infty}(-1)^k J_{2k+1}(x)(4\pi P_{\Delta\phi,\Delta\theta}(\Delta\phi, \Delta\theta) \\ & \div x(J_0(\phi) + 2\sum_{k=1}^{\infty}(-1)^k J_{2k}(\phi))) \\ & \otimes 4P^{ze}_{\Delta\theta max}J_0\left(kd_z(b-b')\right) \end{aligned} \quad (25)$$

III. THREE DIMENSIONAL MIMO CHANNEL MODELING

In this section, we analyze WINNER+ and 3GPP standard which follows a geometry-based stochastic channel approach in [20] and [23] and presents the relating channel realization between the BS and the mobile station (MS). We considered this WINNER+ and 3GPP standard because it has been acknowledged through research that there is a substantial component of energy that is radiated in the elevation. Therefore, describing the propagation paths in the azimuth does not enhance performance [2]. Furthermore, unlike the 2D 3GPP model where the antenna boresight is fixed, and the channel's degrees of freedom in the elevation is not being exploited, the WINNER+ and 3GPP standard under consideration present the elevation angle of the antenna boresight, θ_{tilt}, into the channel equation [2]. Consequently, the dynamic variation of the downtilt angles can uncover several potentials for 3D beamforming that can lead to significant performance improvements [2].

To accomplish the objective of this paper, we modeled the BS as CA and URA. According to [20], the effective 3GPP channel between s^{th} BS antenna ports and u^{th} MS antenna port is expressed as

$$\begin{aligned} [H_{s,u}] = {} & \sum_{n=1}^{N}\alpha_n\sqrt{g_t(\phi_n, \theta_n, \theta_{tilt})}\sqrt{g_r(\varphi_n, \vartheta_n)} \\ & \times [a_r(\varphi_n, \vartheta_n)]_u \times [a_t(\phi_n, \theta_n)] \end{aligned} \quad (26)$$

where $s = 1, ..., N_{BS}$, $u = 1, ..., N_{MS}$, α_n is the complex amplitude of the n^{th} path, (ϕ_n, θ_n) are the azimuth and elevation angles-of-departure (AODs), respectively. (φ_n, ϑ_n) are the azimuth and elevation angles of arrival (AOAs) of the n^{th} path respectively. Following the procedures of ITU and 3GPP standards, the gain of each antenna array at the BS is expressed as $g_t(\phi_n, \theta_n, \theta_{tilt}) \approx g_{t,H}(\phi_n g_{t,V}(\theta_n, \theta_{tilt}))$. The antenna array responses are represented by $a_t(\phi, \theta)$ and $a_r(\phi, \theta)$. The linear expression of the horizontal and vertical antenna patterns at the BS can be expressed as [23] and [27]

$$g_{t,H}(\phi) = -12(\phi/\phi_{3dB})^2 dB \quad (27)$$

$$g_{t,V}(\theta, \theta_{tilt}) = (\theta - \theta_{tilt}/\theta_{3dB})^2 dB \quad (28)$$

where θ_{tilt} is the downtilt angle of the antenna. ϕ_{3dB} and θ_{3dB} are the horizontal and vertical $3dB$ beamwidths, respectively. Also, the individual radiation pattern at the MS, $g_r(\varphi, \vartheta)$ is taken as $0dB$ since the MS should generally not favour any direction.

Unlike the UCA, the CA configuration in *Figure 2a* is obtained by wrapping a uniform URA around a virtual cylinder. Therefore in this analysis, we modeled the CA as an A-element ULA in the z direction (zenith domain) and B-element on the x, y plane (azimuth domain) just as in [19]. The location vector of the s^{th} transmit (Tx) antenna in the case of the CA can be determined by knowing the position of m^{th} UCA in the z direction and the angular position of the n^{th} element on the m^{th} UCA on the x, y plane, where $m = 1, ..., M$ is the total number of UCA elements in the z direction and $n = 1, ..., N$ is the total number of antenna elements on each UCA. Given the array dimension of the CA as $l = 4\lambda$, the radius of the cylinder and UCA is given as $\rho = 4\lambda/l$ [19]. In addition, if $d_z = 4\lambda/M$ wavelengths is the distance between the first and the second UCA in the z direction, then the position of the third and the subsequent UCA will be $4\lambda(m-1)/M$ wavelengths and so on as shown in *Figure. 2a*. According to [23], the angular position of the n^{th} element of the m^{th} UCA on the x, y plane is $\varphi_s = 2\pi(n-1)/N$ and the location vector can be expressed as $v_t \cdot x_s = \cos(\phi - \varphi_s)\sin\theta$. In consideration of the above assumptions, the array

response of s^{th} BS antenna port of CA using Eq. (26) can be expressed as

$$[a_t(\phi_n, \theta_n)]_s = exp(ik\rho(4\lambda(m-1)/M)\cos(\phi_n - \varphi_s)\sin\theta_n) \tag{29}$$

At the MS, we considered the LTE antenna ports used to support different transmission modes described in [14] and [29]. With this configuration, each antenna port seems like a single antenna, since its elements carry the identical signal. This is because our objective is to determine the channel between the transmitting antenna port and the receiver side. The array response of u^{th} MS antenna port in connection with the 3-D channel model is expressed as [29]

$$[a_r(\varphi_n, \vartheta_n)]_u = exp(ik(u-1)d_r \sin\varphi \sin\vartheta) \tag{30}$$

The resultant 3-D channel realization between s^{th} transmit antenna port of CA and the single antenna receiving (Rx) port can be expressed as

$$\begin{aligned}[H_{s,u}]_{CA} = &\sum_{n=1}^{N} \alpha_n \sqrt{g_t(\phi_n, \theta_n, \theta_{tilt})} \\ &\times \exp(ik\rho(4\lambda(m-1)/M)\cos(\phi_n - \varphi_s)\sin\theta_n) \\ &\times \sqrt{g_r(\varphi_n, \vartheta_n)}\exp(ik(u-1)d_r \sin\varphi \sin\vartheta)\end{aligned} \tag{31}$$

where k is the wave number, d_r is the separation between the receiving antenna ports.

In the case of URA shown in *Figure 2b*, on the scalars z and y-axes [3],

$$Z = \sqrt{Z_z^2 + Z_y^2}, \quad Z_z = 2\pi dz(n-m)/\lambda,$$

$Z_y = 2\pi dy(p-q)/\lambda$ and $\varphi_s = \cos^{-1}(Z_z/Z_y)$ The position of elements at the transmitter is defined by $Z\angle\varphi$ and the location vector of s^{th} transmit element for URA can be expressed as $v_t.x_s = \cos(\phi - \varphi_s)\sin\theta$. In view of the above assumptions, the array response of s^{th} BS antenna port of URA regarding Eq. (26) can be expressed as

$$[a_t(\phi_n, \theta_n)]_s = \exp(ikZ\cos(\phi_n - \varphi_s)\sin\theta_n) \tag{32}$$

Therefore, the 3-D channel realization between s^{th} transmit antenna port of URA and the u^{th} receiving port regarding Eq.(26) is given by

$$\begin{aligned}[H_{s,u}]_{URA} = &\sum_{n=1}^{N} \alpha_n \sqrt{g_t(\phi_n, \theta_n, \theta_{tilt})} \\ &\times \exp(ikZ\cos(\phi_n - \varphi_s)\sin\theta_n) \\ &\times \sqrt{g_r(\varphi_n, \vartheta_n)}\exp(ik(u-1)d_r \sin\varphi \sin\vartheta)\end{aligned} \tag{33}$$

IV. SYSTEM MODEL

In this paper, we consider the DL system model described in [13] where the link is established between a N_{BS} antenna BS and an M single antenna receivers. We presume that the uplink (UL) pilots of the MIMO with N_{BS} transmitting antennas enable the BS to estimate the DL channel. In addition, we assume conventional time division duplex (TDD) described in [13], where each channel is static for a coherence period of T_{coher} for the useful channel and any interfering channels. The T_{coher} of each block fading structure is divided into phases for UL and DL pilot and data transmission. Following the guidelines in [13], we present a correlated receive signal model at the user equipment (UE) based on and hardware impairments as

$$y = \sqrt{\sigma}G\left(x + \eta_t^{BS}\right) + \eta_t^{UE} + n \tag{34}$$

where η_t^{BS} and η_t^{UE} are the transceiver impairments for the transmitter hardware at the BS and UE, respectively. σ is the transmit signal to noise ratio (SNR), x is the $N_{BS} \times 1$ precoded data vector and n is the independent and identically distributed noise vector. Using the Kronecker model, the estimated channel matrix is expressed as [22]

$$G = R_t^{1/2} H_{su} \tag{35}$$

where R_t is the $N_{BS} \times N_{BS}$ transmit SC matrix. We consider a cross-polarized (x-pol) antenna configuration, with the SC matrix modeled as [19].

$$R_t = X_{pol} \odot R \tag{36}$$

where $N_{BS} \times N_{BS}$ matrix R is the SC matrix and $\odot$ represents the Hadaard product. X_{pol} is the matrix given by [19]

$$X_{pol} = 1_{M/2} \otimes \begin{bmatrix} 1 & \sqrt{\delta} \\ \sqrt{\delta} & 1 \end{bmatrix} \tag{37}$$

where δ is the cross-correlation between the two antenna elements in the X-pol configuration, $1_{M/2}$ is $M/2 \times M/2$ matrix of ones and $\otimes$ is the Kronecker product.

For the channel capacity analysis, we present the DL upper bound capacity to evaluate the proposed SC expression. We examine the uncorrelated DL upper bound capacity (in bits/channel use) limits based on perfect channel state information (CSI) derived in [13] and present a correlated model as

$$\begin{aligned}C^{DL} \leq \frac{T_{data}^{DL}}{T_{coher}} \Big\{ &\log_2 \Big(1 + G_t^{\dagger} \Big(\kappa_t^{BS} D_{|G_t|^2} \\ &+ \kappa_t^{UE} G_t G_t^{\dagger} + R_t \left(\sigma_{UE}^2 / p^{BS}\right)\Big)^{-1} G_t\Big)\Big\}\end{aligned} \tag{38}$$

where $D_{|G|^2} = diag(|G_1|^2, ..., |G_N|^2$, with $G = [G_1, ..., G_N]^T$, p^{BS} is the DL transmit power, κ_t^{BS} and κ_t^{UE} are the impairment parameters at BS and MS, respectively. σ_{UE}^2 is the noise variance. To investigate the effect of correlation on performance, we replaced perfect CSI channel in [13] by the estimated vector G in Eq. (38) and $R_t = I$ for spatially uncorrelated scenario [13], where and I is an identity matrix.

V. NUMERICAL RESULTS

For numerical evaluation, this section validates the effectiveness of the proposed SC expression. In the computation of the SC of CA and URA, we substitute the analytical results in Eqs. (14) and (14) into Eq. (1) and set the AOA cluster means (ϕ, θ) as 0.7 and AOA offset standard deviations (SD), $(\sigma_{\Delta\phi}, \sigma_{\Delta\theta})$ as -0.3 at 2.6 GHz [19], [26]. We assume a total physical space at the transmitter as $l = 4\lambda$ and the maximum radius of $\rho = 2\pi/l$. For the CA, the SC between adjacent ports were analyzed by varying the distance between the antenna elements in the azimuth and zenith domains, respectively. We considered a $2 \times N$ number of elements to compute the correlation coefficient of the CA. This means there are two circular arrays in the zenith domain and $N = 4$ elements on each circular array in the azimuth domain. In the zenith domain, we analyzed the variation between correlation $\left|\rho_{(1,1),(2,2)}\right|$ and d_z, whereas the variation between the correlation $\left|\rho_{(1,2)}\right|$ and d_r was analyzed in the azimuth domain. In the case of the rectangular array, we considered 4×4 array and determined $\left|\rho_{(1,2)}\right|$. As illustrated in *Figures 4 and 5*, there is an excellent agreement between theoretical and simulation results for all cases using Monte-Carlo simulations. This validates the MPA concept as the SC diminishes as the antenna separation increases.

Moreover, it is also clear in *Figures 4 and 5* that the effect of mutual coupling increases the correlation between the antenna elements. However, the effect of mutual coupling reduces as the separation between the antenna elements increases in both azimuth and zenith domains. It was observed that separation of half-wavelength between antenna elements is insufficient to decorrelate the antenna elements, in both domains.

Next, we examine the effects of SC on DL capacity at various signal-to-noise ratio (SNR). We incorporate the effect of correlation into the DL capacity in Eq. (38). The simulated channel is according to Eqs. (25), (35) - (38). To illustrate our concept, the simulation considers ideal transceiver hardware where $\kappa_t^{BS} = \kappa_t^{UE} = 0$ and TDD duplex where $T_{data}^{DL}/T_{coher} = 0.45$. The noise variance is set as $\sigma_{UE}^2 = 10^{-7.9}\mu J$ per channel use and transmit power is taken as $p^{BS} = 0.0222\mu J$ per channel use as in [13]. We generated the channel coefficients using the proposed channel realization between s^{th} transmit antenna port and the u^{th} receiver (Rx) antenna port using Eqs. (31) and (33) in Section III.

For validation purposes, we consider $\theta_{tilt} = 95°$, $\theta_{3dB} = 15°$, and $\phi_{3dB} = 70°$ as in [23] at the BS for the 3-D channel modeling shown in *Figure 3*. Moreover, the multipath delay associated with AOD, multipath components for each AOA, and the power azimuth spectrum (PAS) arriving at the MS are modeled as Laplacian distribution with specific 3GPP standards.

For this study, we illustrate the dependency of the DL capacity on SC for $4 \times N$ transmit antennas, where $N = \{4, 8, 10, 32, 64\}$ for CA and URA at 2.6 GHz. Using the proposed SC expression, we show in *Figures 6 and 7* the

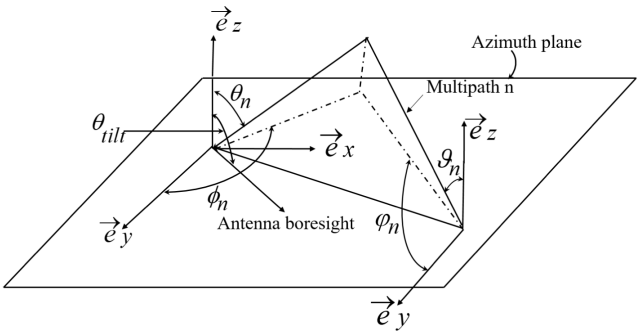

FIGURE 3. 3-D channel model.

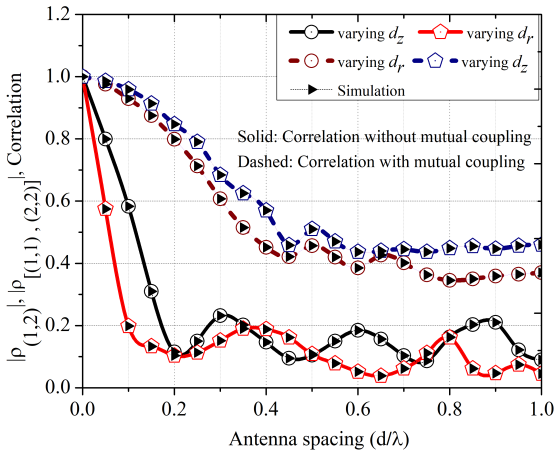

FIGURE 4. SC between adjacent antenna ports using 3GPP measured values for cylindrical array.

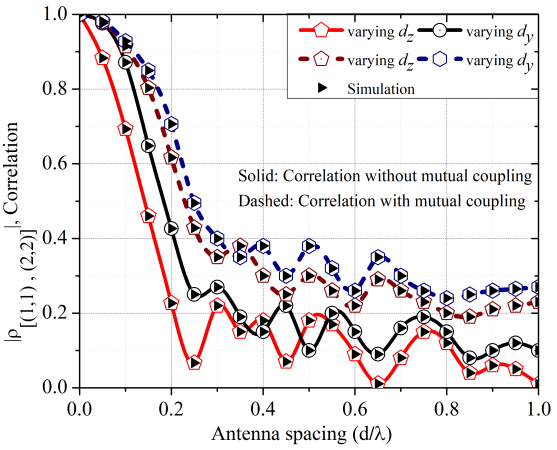

FIGURE 5. SC between adjacent ports using 3GPP measurements for rectangular array.

variations in upper bound capacities regarding the number of BS antennas for fixed SNR of 5 dB, 10 dB and 20 dB.

It can be observed that the effect of correlation on the performance is more significant at a reduced number of BS antennas than an increased number of BS antennas. Results show that increasing antenna elements in a fixed physical

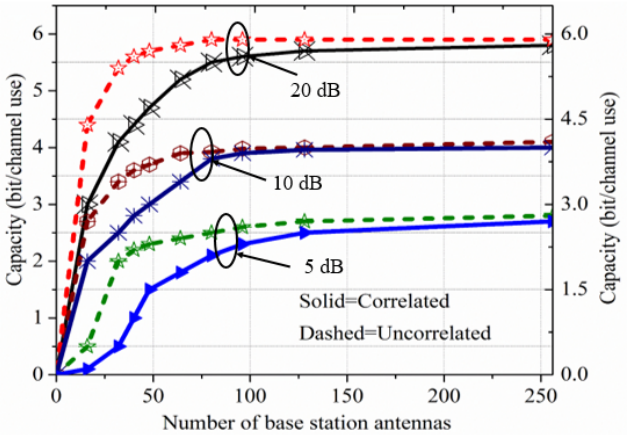

FIGURE 6. Capacity analysis for cylindrical array.

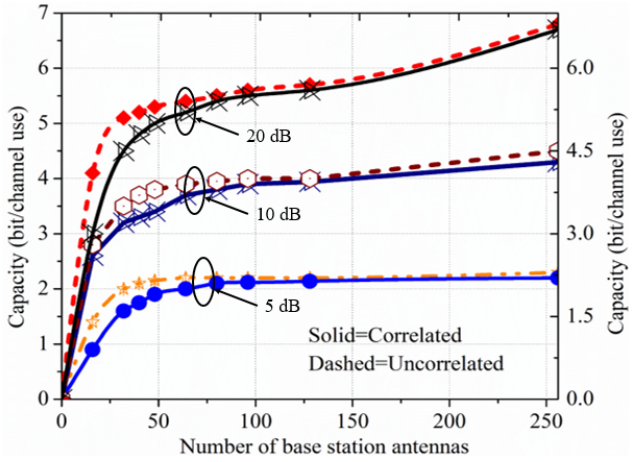

FIGURE 7. Capacity analysis for rectangular array.

space enhances DL capacity performance, regardless of user channels becoming more correlated due to reducing inter-element separation.

Surprisingly, in *Figure 7*, we note that while SC restricts the channel capacity at a reduced number of transmit antennas, this restriction is relaxed as the number of transmit antennas increase, at $N > 20$, for all SNR values. A similar observation was made at $N > 20$ for SNR value at 10 dB for the CA in *Figure 6*. However, at SNR values of 5 dB and 20 dB, a close match in performance between correlated and uncorrelated channel capacity was recorded. This indicates that the restriction on channel capacity by SC is not significant while increasing the transmit antennas elements in massive MIMO system.

Our results support field measurements and result in [13] that in the field of massive MIMO, user channels decorrelate when the number of BS antennas increases and improves performance. This renders the proposed SC expression helpful for generating SC of antenna topologies to evaluate massive MIMO networks. The system parameters utilized in this work are presented in *Table 1*.

TABLE 1. System parameters.

Parameter	Value
Frequency	2.6 GHz
X-pol parameter, $\sqrt{\delta}$	0.1
Azimuth AOD offset PDF, $p_{\Delta,\phi}(\Delta\phi)$	Wrapped Gaussian
Zenith AOD offset PDF, $p_{\Delta,\theta}(\Delta\theta)$	Laplacian
AOD cluster mean, ϕ, θ	0.7
AOD offset SD, $\sigma_{\Delta\phi}, \sigma_{\Delta\theta}$	-0.3
θ_{tilt}	95°
θ_{3dB}	15°
ϕ_{3dB}	70°
T_{data}^{DL}/T_{coher}	0.45
Noise variance σ^2_{UE}	$10^{-7.9}\mu J$/channel
Transmit power p^{BS}	$0.0222\mu J$/channel

VI. CONCLUSION

In this paper, we derived an approximate expression for SC of CA and URA regarding the MPA of offset distribution using cluster model. We have demonstrated the benefits of the MPA concept of characterizing the SC of antenna arrays because regardless of the numerical integration, we obtained a perfect match between theoretical and Monte Carlo simulations. We validated the proposed SC expression in a geometry-based stochastic channel and examined the effect of increasing the BS antennas in a fixed transmitter space. Results illustrate that the downlink capacity is insensitive to the effect of correlation by increasing the number of elements in massive MIMO systems. Even though increasing the number of antenna elements increases correlation. Our outcomes demonstrated that while SC restricts the channel capacity at a reduced number of transmit antennas for both antenna arrays, this restriction was relaxed as the number of transmit antennas increases. It was also observed that separation of more than half-wavelength is required to decorrelate the antenna elements. This supports existing developments that user channels decorrelate as the number of antennas increases in the field of massive MIMO.

REFERENCES

[1] L. Zhao, L. K. Yeung, and K. L. Wu, "A coupled resonator decoupling network for two element compact antenna arrays in mobile terminals," *IEEE Trans. Antennas Propag.*, vol. 62, no. 5, pp. 2767–2776, May 2014.

[2] Q. U. A. Nadeem, A. Kammoun, M. Debbah, and M. S. Alouini, "3D massive MIMO systems: Modeling and performance analysis," *IEEE Trans. Wireless Commun.*, vol. 14, no. 12, pp. 6926–6939, Dec. 2015.

[3] S. K. Yong and J. S. Thompson, "A 3-dimensional spatial fading correlation model for electromagnetic vector sensors," in *Proc. 6th Int. Symp. Antennas, Propag. EM Theory*, Beijing, China, 2003, pp. 843–846.

[4] C. Masouros, J. Chen, K. Tong, M. Sellathurai, and T. Ratnarajah, "Towards massive-MIMO transmitters: On the effects of deploying increasing antennas in fixed physical space," in *Proc. Future Netw. Mobile Summit*, Lisboa, Portugal, 2013, pp. 1–10.

[5] A. Jamil, M. Z. Yusoff, and N. Yahya, "Current issues and challenges of MIMO antenna designs," in *Proc. Int. Conf. Intell. Adv. Syst.*, Kuala Lumpur, Malaysia, 2010, pp. 1–5.

[6] M. Mohajer, G. Z. Rafi, and S. Safavi-Naeini, "MIMO antenna design and optimization for mobile applications," in *Proc. IEEE Antennas Propag. Soc. Int. Symp.*, Charleston, SC, USA, Jun. 2009, pp. 1–4.

[7] C.-X. Wang *et al.*, "Cellular architecture and key technologies for 5G wireless communication networks," *IEEE Commun. Mag.*, vol. 52, no. 2, pp. 122–130, Feb. 2014.

[8] E. G. Larsson, O. Edfors, F. Tufvesson, and T. L. Marzetta, "Massive MIMO for next generation wireless systems," *IEEE Commun. Mag.*, vol. 52, no. 2, pp. 186–195, Feb. 2014.
[9] J. Hoydis, M. Kobayashi, and M. Debbah, "Green small-cell networks," *IEEE Veh. Technol. Mag.*, vol. 6, no. 1, pp. 37–43, Mar. 2011.
[10] W. Liu, S. Han, C. Yang, and C. Sun, "Massive MIMO or small cell network: Who is more energy efficient?" in *Proc. IEEE Wireless Commun. Netw. Conf. Workshops (WCNCW)*, Shanghai, China, Apr. 2013, pp. 24–29.
[11] K. Zheng, S. Ou, and X. Yin, "Massive MIMO channel models: A survey," *Int. J. Antennas Propag.*, vol. 2014, Jun. 2014, Art. no. 848071.
[12] J. Hoydis, S. ten Brink, and M. Debbah, "Massive MIMO: How many antennas do we need?" in *Proc. 49th Annu. Allerton Conf. Commun., Control, Comput. (Allerton)*, Monticello, IL, USA, Sep. 2011, pp. 545–550.
[13] E. Björnson, J. Hoydis, M. Kountouris, and M. Debbah, "Massive MIMO systems with non-ideal hardware: Energy efficiency, estimation, and capacity limits," *IEEE Trans. Inf. Theory*, vol. 60, no. 11, pp. 7112–7139, Nov. 2014.
[14] G. Liu, X. Hou, F. Wang, J. Jin, H. Tong, and Y. Huang, "Achieving 3D-MIMO with massive antennas from theory to practice with evaluation and field trial results," *IEEE Syst. J.*, vol. 11, no. 1, pp. 62–71, Mar. 2017.
[15] A. D. Pluzhnikov, E. N. Pribludova, and A. G. Ryndyk, "Cylindrical array as a means of the clutter suppression via scanning acceleration and space-time signal processing," in *Proc. 44th Eur. Microw. Conf.*, Rome, Italy, 2014, pp. 1864–1867.
[16] Z. Sipus, M. Bosiljevac, and S. Skokic, "Mutual coupling analysis of cylindrical waveguide arrays using hybrid SD-UTD method," in *Proc. IEEE Antennas Propag. Soc. Int. Symp.*, vol. 1A, Jul. 2005, pp. 155–158.
[17] A. Forenza, D. J. Love, and R. W. Heath, Jr., "Simplified spatial correlation models for clustered MIMO channels with different array configurations," *IEEE Trans. Veh. Technol.*, vol. 56, no. 4, pp. 1924–1934, Jul. 2007.
[18] D. Ying, F. W. Vook, T. A. Thomas, D. J. Love, and A. Ghosh, "Kronecker product correlation model and limited feedback codebook design in a 3D channel model," in *Proc. IEEE Int. Conf. Commun. (ICC)*, Sydney, NSW, Australia, Jun. 2014, pp. 5865–5870.
[19] C. T. Neil, M. Shafi, P. J. Smith, and P. A. Dmochowski, "On the impact of antenna topologies for massive MIMO systems," in *Proc. IEEE Int. Conf. Commun. (ICC)*, London, U.K., Jun. 2015 pp. 2030–2035.
[20] *Study on 3D Channel Model for LTE*, document 3GPP TR 36.873 V12.0.0, Sep. 2014.
[21] J. B. Andersen and K. I. Pedersen, "Angle-of-arrival statistics for low resolution antennas," *IEEE Trans. Antennas Propag.*, vol. 50, no. 3, pp. 391–395, Mar. 2002.
[22] A. E. Ampoma, H. Zhang, Y. Huang, G. Wen, and O. G. Kwame, "Three-dimensional spatial fading correlation of uniform rectangular array using total power of angular distribution," *IEEE Antennas Wireless Propag. Lett.*, vol. 16, pp. 2134–2137, 2017.
[23] Q. U. A. Nadeem, A. Kammoun, M. Debbah, and M. S. Alouini, "Spatial correlation characterization of a uniform circular array in 3D MIMO systems," in *Proc. 17th Int. Workshop Signal Process. Adv. Wireless Commun. (SPAWC)*, Edinburgh, U.K., 2016, pp. 1–6.
[24] A. Milton and S. Irene, *Handbook of Mathematical Functions with Formulas, Graphs and Mathematical Tables*. New York, NY, USA: Dover, 1965.
[25] D. Manteuffel, "MIMO antenna design challenges," in *Proc. Antennas Propag. Conf.*, Loughborough, U.K., 2009, pp. 50–56.
[26] *Study on 3D channel Model for LTE (Release 12)*, document V2.0.0, 3rd Generation Partnership Project; Technical Specification Group Radio Access Network, Mar. 2014.
[27] *Guidelines for Evaluation of Radio Interface Technologies for IMT-Advanced*, document ITU-R M.2135, 2008. [Online]. Available: http://www.itu.int/pub/R-REP-M.2135-2008/en
[28] J. L. Burbank, J. Andrusenko, J. S. Everett, and W. T. M. Kasch, *Wireless Networking: Understanding Internetworking Challenges*. Piscataway, NJ, USA: IEEE Press, 2013.
[29] A. Kammoun, H. Khanfir, Z. Altman, M. Debbah, and M. Kamoun, "Preliminary results on 3D channel modeling: From theory to standardization," *IEEE J. Sel. Areas Commun.*, vol. 32, no. 6, pp. 1219–1229, Jun. 2014.
[30] E. Bjornson, J. Hoydis, M. Kountouris, and M. Debbah, "Simulation code for massive MIMO systems with non-ideal hardware: Energy efficiency, estimation, and capacity limits," *IEEE Trans. Inf. Theory*, vol. 60, no. 11, pp. 7112–7139, Nov. 2014. [Online]. Available: https://ebjornson.com/research/
[31] A. Paulraj, R. Nabar, and D. Gore, *Introduction to Space-Time Wireless Communications*, 1st ed. Cambridge, U.K.: Cambridge Univ. Press, 2003.
[32] A. E. Ampoma, G. Wen, H. Zhang, Y. Huang, O. K. Gyasi, and P. I. Tebe, "3D correlation function of a uniform circular array using maximum power in the direction of arrival," in *Proc. Prog. Electromagn. Res. Symp.-Fall (PIERS-FALL)*, Singapore, 2017, pp. 2996–3003.

AFFUM EMMANUEL AMPOMA received the B.S. degree in electronics and communication engineering from the Kwame Nkrumah University of Science and Technology, Kumasi, Ghana, in 2007, and the M.Tech. degree in communication system from SRM University, Chennai, India. He is currently pursuing the Ph.D. degree with the Center for RFIC and System Technology, School of Communication and Information Engineering, University of Electronic Science and Technology of China. He is also with the Department of Electrical and Electronic Engineering, Kwame Nkrumah University of Science and Technology. His current research interests include in the field of wireless communication and signal processing with a particular focus on array processing, channel modeling, and performance analysis of wireless communication systems.

GUANGJUN WEN received the B.Sc. and M.Eng. degrees from Chongqing University, Chongqing, China, in1986 and 1992, respectively, and the Ph.D. degree the University of Electronic Science and Technology of China (UESTC), Chengdu, China, in 1998. From 1986 to 1995, he was with Chongqing University, as a Lecturer. He was with UESTC, from 1998 to 2000, and then with the Electronics and Telecommunication Research Institute, South Korea, from 2000 to 2001, as a Post-Doctoral Fellow. He was with Nanyang Technological University, Singapore, as a Research Fellow from 2001 to 2002. He was with VS Electronic Pte Ltd., Singapore, and the Sumitomo Electric Group, Yokohama, Japan, as a Senior RF Design Engineer, from 2002 to 2005. Since 2004, he has been a Full Professor at UESTC. He has authored or co-authored over 200 journal papers and presented over 120 conference papers. His research interests are in radio frequency integrated circuits and systems for various wireless communication systems, analysis and design of RFID tag and reader, circuit components, and antennas design for the Internet of Things.

YONGJUN HUANG received the M.S. and Ph.D. degrees from the University of Electronic Science and Technology of China (UESTC), Chengdu, China, in 2010 and 2016, respectively. From 2013 to 2015, he was a Visiting Scholar with the Department of Solid-State Science and Engineering, and Mechanical Engineering, Columbia University, New York City, NY, USA, and a Visiting Project Scientist with the Department of Electrical Engineering, University of California at Los Angeles, Los Angeles, CA, USA. He is currently an Assistant Professor with UESTC. His research interests include antennas, microwave passive components, electromagnetic metamaterials, chip-scale photonic crystal cavity optomechanics, low phase noise RF sources, and high-resolution force/field.

KWAME OTENG GYASI was born in Kumasi, Ghana, in 1989. He received the B.Sc. degree in telecommunication engineering from the Kwame Nkrumah University of Science and Technology, Kumasi, in 2011, and the M.Sc. degree in communication and information engineering from the University of Electronic Science and Technology, Chengdu, China, in 2014. He is currently pursuing the Ph.D. degree in information and communication engineering with the University of Electronic Science and Technology of China. He was a Teaching Assistant with the Kwame Nkrumah University of Science and Technology from 2011 to 2012. During this time, he aided in teaching courses, like electromagnetic compatibility, antennas and propagation, and telecom policy. His research interests include electromagnetic field theory, circularly polarized antennas, printed wideband antennas, planar monopole antennas, and slot antennas.

PARFAIT I. TEBE received the B.Sc. degree in telecommunication engineering from the Ghana Telecom University College, Ghana, in 2011, and the M.Eng. degree in communication and information engineering from the University of Electronic Science and Technology of China (UESTC), China, in 2014. He is currently pursuing the Ph.D. degree in communication and information engineering at UESTC. His current research interests focus on massive MIMO. He is a Student Member of IEICE.

KWADWO NTIAMOAH-SARPONG received the B.Sc. degree in electrical and electronic engineering from the Kwame Nkrumah University of Science and technology, Ghana, in 2005, and the master's degree in telecommunication management from the Han University of Applied Science, The Netherlands, in 2011. He is currently pursuing the Ph.D. degree with the School of Communication and information Engineering, University of Electronic Science and Technology of China, Chengdu, China. His main research interests are wireless communications and networking, radio resource management, and 5G.